

**RIGA TECHNICAL UNIVERSITY**  
Faculty of Electronics and Telecommunications  
Department of Transport Electronics and Telematics

**Elans GRABS**

Doctoral Student of the Programme  
“Computer Control, Information and Electronic Systems of Transport”

**SELF-SIMILAR TRAFFIC PARAMETER  
ANALYSIS FOR NETWORK PERFORMANCE  
IMPROVEMENT BY USING REAL-TIME  
DISCRETE WAVELET TRANSFORM**

Summary of the Doctoral Thesis

Scientific supervisor  
Professor, *Dr. habil. sc. ing.*  
**E. PETERSONS**

**RTU Press**  
**Riga 2016**

Grabs E. Self-Similar Traffic Parameter Analysis for  
Network Performance Improvement by Using Real-Time  
Discrete Wavelet Transform.  
Summary of Doctoral Thesis. – Riga: RTU Press, 2016. –  
30 p.

Printed according to the Resolution of ETF Promotion  
Council “RTU P-08” dated by 21 January 2016 with No. 31.



The present research has been supported by the European Social Fund within the project  
“Support for the Implementation of Doctoral Studies at Riga Technical University”.

**DOCTORAL THESIS PROPOSED TO RIGA TECHNICAL UNIVERSITY FOR  
THE PROMOTION TO THE SCIENTIFIC DEGREE OF DOCTOR OF  
ENGINEERING SCIENCES**

To be granted the scientific degree of Doctor of Engineering Sciences, the present Doctoral Thesis will be defended on 5 May 2016, at the Faculty of Electronics and Telecommunication, Riga Technical University, Azenes Street 12, Room 2-38.

OFFICIAL REVIEWERS:

Professor *Dr. sc. ing.* Gunars Lauks  
Riga Technical University, Latvia

Professor *Dr. sc. ing.* Guntis Barzdins  
University of Latvia, Latvia

Professor *Dr. sc. ing.* Aleksandrs Grakovskis  
Transport and Telecommunication Institute, Latvia

DECLARATION OF ACADEMIC INTEGRITY

I hereby declare that the Doctoral Thesis submitted for the review to Riga Technical University for the promotion to the scientific degree of Doctor of Engineering Sciences is my own and does not contain any unacknowledged material from any source. I confirm that this Thesis has not been submitted to any other university for the promotion to other scientific degree.

Elans Grabs .....(Signature)

Date: .....

The Doctoral Thesis has been written in Latvian and includes introduction, 4 chapters, conclusions, bibliography and 16 appendices. It has been illustrated by 76 figures. The total volume of the present Thesis is 200 pages, including appendices (129 pages without appendices). The bibliography contains 100 reference sources.

# TABLE OF CONTENTS

<b>1. Generalized Description of the Doctoral Thesis</b>	<b>5</b>
1.1 Topicality of the Research . . . . .	5
1.2 Aims of the Doctoral Thesis . . . . .	6
1.3 Scientific Novelty and Main Results . . . . .	6
1.4 Thesis Statements to Be Defended . . . . .	7
1.5 Research Methodology . . . . .	7
1.6 Practical Application of Research Results . . . . .	8
1.7 Approbation of the Results . . . . .	8
1.8 Structure of the Doctoral Thesis . . . . .	9
<b>2. Detailed Descripton of the Doctoral Thesis</b>	<b>10</b>
2.1 Self-Similar Traffic Model and Discrete Wavelet Transform . . . . .	10
2.2 Real-Time Discrete Wavelet Transform with Filter Banks . . . . .	12
2.3 Traffic Self-Similarity Parameter Estimation, Implementation with Filter Banks and Estimation Error . . . . .	15
2.4 Packet Loss Probability Analysis for Generated Self-Similar Traffic in $P/M/1/K$ and $G/M/1/K$ Simulation Models . . . . .	20
<b>Main Conclusions</b>	<b>26</b>
<b>References</b>	<b>28</b>

# 1. Generalized Description of the Doctoral Thesis

## 1.1 Topicality of the Research

At present, it is widely assumed that modern network traffic has self-similarity properties, which means the network traffic flow has similar behaviour at different scales (seconds, minutes, hours). This was confirmed a long time ago by [16]; the authors conducted traffic measurements in different *Bellcore* laboratory local networks during the period between 1989 and 1992. The work described how data packets were collected over short time intervals and probability distributions obtained. Such distributions were studied at lower scales by decreasing packet count time interval by 10 times for random distribution subinterval.

Self-similarity concept is closely related to chaos and fractals theory and power series. The first scientist, who noticed such a phenomena, was Benua Mandelbrot. He proposed the mathematical means to describe complex forms of nature [20], more specifically – the fractals, which are widely encountered in a world around us. The self-similar process seems to be the same (or it has the same behaviour) at different scales. The scales can be represented by space coordinates or time coordinate. The quantitative measure of self-similarity is the Hurst parameter.

There are different methods for Hurst parameter estimation and research has been performed for comparison of the precision of such methods, for example in [6], [32]. The Hurst parameter evaluation can be performed by different transforms – fractional Fourier transform [33], empirical mode decomposition (EMD) [10], discrete wavelet transform [1]. The latter, considering its applicability for scale invariance, has been used in the present research. Thus, in order to estimate the Hurst parameter in real-time, the real-time discrete wavelet transform algorithm is required. Such algorithms exist and are described in works, such as [21]. The transform can be performed at low computation costs by using filter banks [28].

The self-similarity is strongly expressed in modern networks. Despite the fact that old methods based on Poisson distribution and Markov processes cannot describe modern traffic [18], they still can be used in addition to modern methods to analyse traffic more precisely [27]. Interesting to note that traffic can be self-similar not only in computer networks – for example, [9] describes self-similar traffic in integral circuits (complex ICs, such as DSP). Thus, it is important to estimate the measure of self-similarity by evaluating the Hurst parameter. The present research describes such an approach based on discrete wavelet transform, which has been for the first time proposed in [1]. This work has encouraged interest of many researchers regarding this topic and it has been continued to design even better estimator based on discrete wavelet transform. For example, in [17] it has been discovered that the number of wavelet vanishing moments <sup>1</sup> does not necessarily increase estimation accuracy for the Hurst parameter. The discrete wavelet transform for estimation of the Hurst parameter is still a topical issue, which has been proved by latest publications, in which new wavelets are discovered for estimation accuracy improvement. For example, [22] describes complex wavelet basis functions.

For such traffic it is important to create control systems to manage network resources more efficiently. There are many studies performed in this field. In order to manage traffic congestions,

---

<sup>1</sup> $M$  vanishing moments for wavelet basis function are defined by generating polynomial of degree  $M - 1$ , for which basis function is orthogonal. The more such moments are, the more accurate and complete description of signal such basis provides.

the traffic can be divided into several classes with different QoS requirements and priorities. In such a way the operation of the network can be optimised [14]. The traffic classifier can be based on the Hurst parameter value estimation as well, as it has been proposed in [24]. The serious research on traffic classification by means of discrete wavelet transform has been made in [26]. Moreover, the number of such classes increases rapidly and it is necessary to create new mechanisms to manage connections (Connection Admission Control, CAC [31], [11], [30]). The topical issue is buffer memory management to control the length of the queue by using various algorithms [3], [2], [7].

The studies show that the Hurst parameter of network traffic depends on a user, requirements and time distribution spent in network connection. It has been attempted to determine, whether the Hurst parameter can be forecast for several days over previous few days in [13] by researching the Internet connection delays. The research results show that such periodicity does indeed exist and there is great difference in the Hurst parameter values during daytime and night-time.

Considering all studies mentioned above, the wavelet transform approach provides various possibilities for traffic analysis and Hurst parameter estimation; it allows classifying traffic types (including by the Hurst parameter), forecasting network traffic [29]. Moreover, discrete wavelet transform can be used for other network related purposes as well – both in wired and in wireless networks. For example, there is an algorithm proposed for detection of WPS attacks in wireless networks [23]. By combining discrete wavelet transform with neuron networks [8], it has been proposed to forecast the required volume of resources in mobile Ad-hoc networks.

Overall, the literature analysis shows that traffic self-similarity is still a topical issue and discrete wavelet transform can be used in many applications for classification, measurement and control of such traffic.

## 1.2 Aims of the Doctoral Thesis

The main aim of the Doctoral Thesis is adaptive processing of traffic according to self-similarity parameter measurements for various network processing node parameters. In order to achieve this aim, the following tasks can be specified:

1. to study real-time discrete wavelet transform implementation techniques and implement such transform with the purpose of network traffic parameter evaluation;
2. to design self-similarity parameter estimator, which can be used to determine the magnitude of traffic self-similarity and change accordingly parameters of network processing node;
3. to study the influence of network processing node buffer memory limit on self-similar network traffic packet loss probability for various self-similarity parameter and utilisation coefficient values;
4. to perform multi-parameter optimisation by using a dynamic programming approach, considering real costs of channel bandwidth and buffer memory.

## 1.3 Scientific Novelty and Main Results

Having conducted the research, the following results, not mentioned in literature, have been obtained:

1. In The Doctoral Thesis, the discrete wavelet transform real-time algorithm implementation has been performed by using filter banks in high-level programming language (in this case C++). The main difference from existing solutions is absence of strict hardware

implementation and no segmentation is needed either, which is the case for most of existing algorithm software implementations.

2. Based on implementation mentioned above, the process (numerical sequence) self-similarity parameter estimator has been implemented, which processes every input process sample separately and, unlike existing solutions, can be used for network routers to estimate the traffic self-similarity parameter.
3. The results of simulation series show that accuracy of self-similarity parameter estimation depends not only on the number of scales for discrete wavelet transform (as it has already been published in literature) but also on the value itself, which is being estimated.
4. The simulation data have been collected and analysed for self-similar traffic with various values of self-similarity parameter, utilisation coefficient, buffer memory volume, number of scales for discrete wavelet transform. Such results can be used for adaptive traffic control or resource distribution scheme implementation in network routers.

## 1.4 Thesis Statements to Be Defended

The Doctoral Thesis presents the following theses:

1. Studies indicate that saving odd-numbered coefficient during discrete wavelet transform downsampling operation reduces time delay of reconstructed signal after inverse discrete wavelet transform.
2. It was observed that optimum number of scales exist for Hurst parameter estimation with discrete wavelet transform, which depends on measured Hurst parameter value and specified maximum number of scales for discrete wavelet transform.
3. The Doctoral Thesis reveal that traffic with the Hurst parameter value  $H = 0.8$  has lower packet loss probability and lower estimation error compared to traffic types with different values of the Hurst parameter.

## 1.5 Research Methodology

In order to accomplish specified tasks, the set of methods should be used, including, but not limited to:

- Literature and reference analysis for deeper research of the issue, evaluation of existing solutions and determination of less studied aspects;
- Theoretical analysis – to prove experimental or simulation data, to determine and explain observation causes, to search for relationships in the obtained simulation results;
- Computer simulation – simulation model creation and research, by repeating simulation with various model parameters and summarisation of the results. The simulations have been performed in *Matlab* and *Simulink* environments;
- Measurements – in order to estimate computational efficiency of calculating algorithms and traffic parameters estimation errors;
- Multi-parameter optimisation – in order to find compromise for network processing node resource distribution with self-similar traffic, specified constraints and total costs.

## 1.6 Practical Application of Research Results

The algorithms presented in the Doctoral Thesis have been designed for microprocessor/microcontroller systems, which can perform discrete wavelet transform in real-time with filter banks and estimate from transform coefficients the magnitude of process self-similarity – the Hurst parameter. Such algorithms can be implemented in routers in order to evaluate the parameters of incoming network traffic and classify different types of traffic with further separate QoS service of these traffic types. Discrete wavelet transform algorithm can be applied in other tasks as well, which are not related to traffic analysis and require evenly time-distributed processing time of minimal value.

## 1.7 Approbation of the Results

The results obtained within the framework of the Doctoral Thesis have been presented at the following international conferences:

1. The 16th International Conference of ELECTRONICS, Palanga, Lithuania, 2012.
2. The 5th International Conference on Information Systems and Technologies, Istanbul, Turkey, 2015.
3. The 7th International Computational Intelligence, Communication Systems and Networks, Riga, Latvia, 2015.
4. Advances in Wireless and Optical Communications, RTUWO'2015, Riga, Latvia, 2015.
5. The 3rd IEEE Workshop on Advances in Information, Electronic and Electrical Engineering AIEEE'2015, Riga, Latvia, 2015.

The research results have been published in the following scientific publications:

1. Grabs, E., Sarkovskis, S. Real-Time Estimation of Traffic Self-Similarity Parameter in Simulink with Wavelet Transform. *Electronics and Electrical Engineering*, 2013, vol. 9, no. 3, pp. 88–91;
2. Asars, A., Grabs, E., Petersons, E. Analysis of Wavelet Estimation of Self-Similar Traffic Parameters in the Simulink Model. *Automatic Control and Computer Sciences*, 2013, vol. 47, no. 3, pp. 132–138;
3. Grabs, E., Petersons E., Optimal Strategy Modelling for Routers Resources Allocation in Self-Similar Traffic Environment. *7-th International Conference on Computational Intelligence, Communication Systems and Networks Proceedings*, Latvia, Riga, 2015, pp. 70–74\*;
4. Bogdanovs, N., Grabs, E., Petersons, E. Software Implementation of Real-time Discrete Wavelet Transform Algorithm with Filter Banks for Network Traffic Parameters Estimation. *The 5th International Conference on Information Systems and Technologies (ICIST2015) Istanbul, Turkey, 21–23 March 2015 Proceedings*, 2015, pp. 1–7;
5. Grabs. E., Petersons, E. Hurst Parameter Estimation with Wavelet Transform by Filter Banks for Matlab Generated Traffic. *Automatic Control and Computer Sciences*, 2015, vol. 49, no. 5, pp. 286–292;
6. Grabs, E., Petersons, E. Software Implementation of Real-time Hurst Parameter Estimator Algorithm with Filter Banks. *Advances in Wireless and Optical Communications 2015, Latvia, Riga, 2015*, pp. 78–81\*;

7. Grabs, E., Petersons, E. Analysis of Self-similar Traffic Parameters for Network Performance Improvement with Real-time Discrete Wavelet Transform. Advances in Information, Electronic and Electrical Engineering, AIEEE'2015, Latvia, Riga, 2015, pp. 1–6\*;
8. Асарс, А., Грабс Э., Петерсонс Э. Анализ Вейвлет-Оценивания Параметров Самоподобного Трафика Модели Simulink. Автоматика и Вычислительная Техника, 2013, vol. 47, no. 3, с. 28–36\*\*;
9. Граб, Э., Петерсонс Э. Оценка Параметра Херста с Помощью Вейвлет-Преобразования и Банка Фильтров для Генерированного в Среде Matlab Трафика. Автоматика и Вычислительная Техника, 2015, vol. 49, no. 5, с. 47–56\*\*.

\* *IEEEExplore* indexed publications.

\*\* Published in Russian, English translations are 2nd and 5th respectively.

The results have been used in the project: National research programme: “DEVELOPMENT OF INNOVATIVE MULTIFUNCTIONAL MATERIALS, SIGNAL PROCESSING AND INFORMATION TECHNOLOGIES FOR COMPETITIVE KNOWLEDGE INTENSIVE PRODUCTS”, Project No 2: “Innovative Signal Processing Technologies for Smart and Effective Creation of Electronic Systems”.

## 1.8 Structure of the Doctoral Thesis

The contents of the Doctoral Thesis are divided in four chapters.

The first chapter provides a theoretical review on traffic self-similarity in computer networks, its influence and causes. The chapter includes the literature analysis, which describes the achieved work in traffic analysis, self-similarity parameter measurements and application, as well as discrete wavelet transform application for network traffic. The basics of discrete wavelet transform are also described in this chapter. The chapter concludes with the self-similar network queuing model analysis in *Simulink* with a self-similarity estimator block.

The second chapter describes discrete wavelet transform practical implementation in high-level programming language C++. The literature review is also available, which justifies a necessity of such algorithm design. There are multiple implementations proposed for direct and inverse discrete wavelet transform with filter banks: direct, polyphase and lattice structures.

The third chapter contains research on self-similarity (Hurst) parameter estimation with discrete wavelet transform and accuracy of such estimation. There are series of simulations made and results have been summarised in tables. Multiple relationships have been studied, as well as a number of required transform scales and traffic window length have also been researched. The chapter concludes with a self-similarity parameter estimator algorithm based on discrete wavelet transform with filter banks and implementation of such algorithm in C++ programming language.

The fourth chapter contains series of simulations with research of self-similarity parameter influence on network processing node buffer memory volume and packet loss probability. The chapter concludes with a queuing system optimisation task solution by using a dynamical programming method with the purpose to minimise total costs for specified packet loss probability value achievement at different values of self-similarity parameter values.

The conclusion of the Doctoral Thesis summarises main results and conclusions of the Doctoral Thesis. Appendices contain modelling results and algorithm implementation source codes related to the Doctoral Thesis contents.

## 2. Detailed Description of the Doctoral Thesis

### 2.1 Self-Similar Traffic Model and Discrete Wavelet Transform

In the field of computer networks, it is often necessary to forecast results of specific changes in network, for example, an increase of the utilization coefficient. In other cases, it is necessary to create a project of the computer network matching specific requirements. In all cases, the performance of system is of great interest – depending on a specific task, this performance can be evaluated as response time, channel bandwidth or other parameters. In order to estimate performance of the system, forecasting mechanisms must be used, and such a problem can be solved by analytical models of queuing theory [35]. Note that the mathematical apparatus of the queuing theory itself is rather complex, but in many cases the practical application of this theory is easy enough.

In modelling of the queues, the main assumptions are given by *Kendall's notation* as follows:  $X/Y/N/K$ , where  $X$  specifies distribution law of request inter-arrival time,  $Y$  specifies distribution law of processing time,  $N$  is the number of processing units and  $K$  is the volume of buffer memory, which determines maximal queue length. Thus, model  $P/M/1/K$  consists of a single processing unit, time intervals between requests are Pareto distributed, processing time is exponentially distributed and buffer memory volume is  $K$  units<sup>2</sup>. The structure of such simplest model is shown in Fig. 1.1.

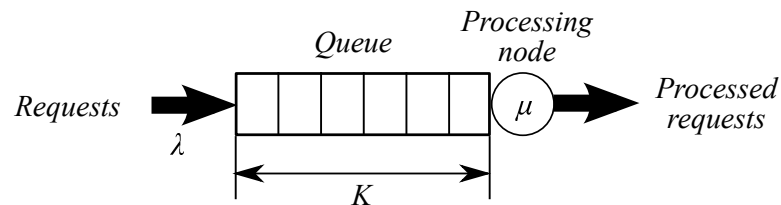


Fig. 1.1. The simplest queuing model with one processing unit.

In order to generate self-similar traffic in simulations, it is required to determine model parameters – intensity of requests  $\lambda$  and self-similarity parameter  $H$ . In case of Pareto distributed process, the probability density function is:

$$f(x) = \frac{\alpha}{\beta} \left( \frac{\beta}{x} \right)^{\alpha+1}, \quad (1.1)$$

where distribution parameters can be evaluated as follows:

$$\alpha = 3 - 2H, \quad (1.2)$$

$$\beta = \frac{\alpha - 1}{\alpha \lambda}, \quad 1 \leq \alpha \leq 2. \quad (1.3)$$

---

<sup>2</sup>For instance, in case of network traffic one packet can be considered to be such a unit.

According to the diagram shown in Fig. 1.1, the *Simulink* model has been created, which evaluates length of the queue and its average value for different self-similarity (Hurst) parameter  $H$  and utilisation coefficient  $\rho$  values. The total number of requests in the queuing system for all experiments is about  $2 \cdot 10^6$  units. Self-similarity parameter values were changed from  $H = 0.5$  to  $H = 0.9$  with step of 0.1 and last value  $H = 0.99$ , which corresponded to a process with the highest self-similarity measure.

The modelling results consisting of *Simulink* data were summarised for every value of utilisation coefficient  $\rho$  in the range from 0.5 to 1.0 for all values of Hurst parameter  $H$ . These values were summarised in multiple tables, such as Table 1.1:

Table 1.1. Comparison of Queue Length  $K$  for Utilisation Coefficient  $\rho = 0.5$

	<i>Simulink</i>	<i>GPSS</i>	Average	Calculated
<b>H = 0.5</b>	0.29 (15)	0.29 (12)	0.39	1.00
<b>H = 0.6</b>	0.35 (18)	0.35 (15)	0.5	1.19
<b>H = 0.7</b>	0.49 (21)	0.49 (17)	0.73	1.59
<b>H = 0.8</b>	0.88 (28)	0.87 (25)	1.41	2.83
<b>H = 0.9</b>	4.02 (86)	3.94 (81)	7.08	16.00
<b>H = 0.99</b>	$2.46 \cdot 10^5$ ( $4.41 \cdot 10^5$ )	$9.91 \cdot 10^5$ ( $2.004 \cdot 10^6$ )	$2.38 \cdot 10^5$	$5.63 \cdot 10^{14}$

The recommended volume of buffer memory  $K_{\text{buf}}$  according to [35] is calculated using (1.4):

$$K_{\text{buf}} = \frac{\rho^{\frac{1}{2(1-H)}}}{(1-\rho)^{\frac{H}{(1-H)}}}. \quad (1.4)$$

By analysing results in the tables, it can be observed that (1.4) in analytical expression cannot be applied, since this formula does not account for packet loss probability  $P_{\text{loss}}$ , which greatly influences buffer memory volume.

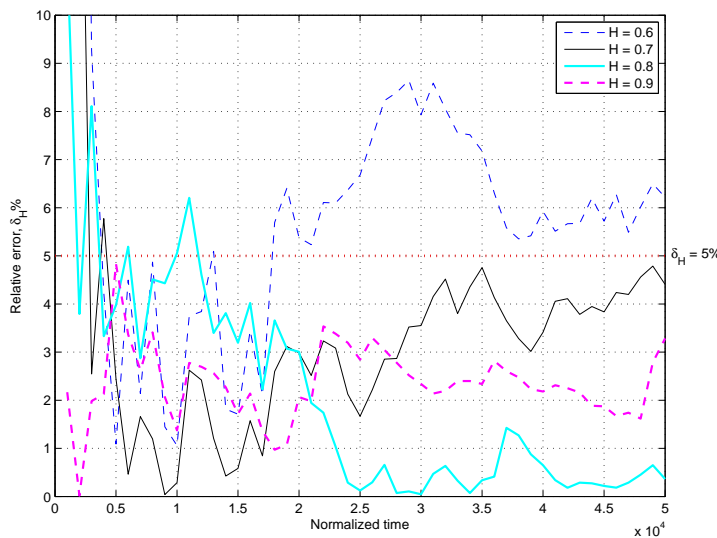


Fig. 1.2. Self-similarity parameter estimation  $E[\hat{H}[n]]$  relative error in percentage relative to source specified value  $H$  for utilisation coefficient  $\rho = 0.8$ .

The created model was further improved by adding the Hurst parameter estimator, described in Chapter 3. This estimator evaluates momentary value  $\hat{H}$  and average value  $E[\hat{H}]$  of the Hurst

parameter. For an average value, the relative error was determined:

$$\delta \hat{H} = \frac{|\hat{H}_{\text{avg}}[n] - H|}{H} \cdot 100, \%. \quad (1.5)$$

The errors calculated according to (1.5) for all values of  $H = \{0.6 \ 0.7 \ 0.8 \ 0.9\}$  are shown in Fig. 1.2 with 5 % interval. Overall, we can observe that for lower values of  $H$  parameter the deviation of  $\hat{H}_{\text{avg}}[n]$  estimates is higher; however, in all cases the self-similarity parameter estimate asymptotically approaches a specified source value. It seems that this time interval does not depend on actual value of self-similarity parameter  $H$ .

## 2.2 Real-Time Discrete Wavelet Transform with Filter Banks

The analysis of literature shows that multi-scale discrete wavelet transform implementation for real-time transform calculation has not been sufficiently researched. There are no such algorithms, which could be applied for self-similarity parameter estimation in real-time. Note that only algorithms processing every traffic sample on all scales are of specific interest here, avoiding segment accumulation and further processing of entire segment.

That is, mostly, the way in which discrete wavelet transform algorithm is available in literature – it is based on Mallat pyramidal filter bank algorithm [19] that is well described in many theoretical sources (for example, [28]). According to this algorithm, the data segment is accumulated with further processing by  $j = 1$  scale filter bank (the entire segment at once), afterwards the resulting approximation coefficients are processed by  $j = 2$  scale filter bank, and so on. Such an approach can be successfully used in real-time processing, as it has been shown in Master’s Thesis [5] for audio signal real-time processing. Many other studies describe segmentation – with or without overlapping to reduce border-effect of the segmentation (for example, [25]).

However, if discrete wavelet transform is calculated by filter bank approach (see Fig. 2.1(a)), the first real results can be used at once, before the whole segment has been processed, if operation of these filters is implemented directly by means of software, without calculation of discrete convolution for the entire data segment. It is possible, since the transform procedure itself by its nature is none other than a digital filtering operation, which can be performed in real-time. Moreover, in case of wavelet transform very often non-recursive digital filters are used with finite impulse response length; thus, time delay before the first result can be estimated and has low values.

Fig. 2.1(a) shows discrete wavelet transform for 1 scale with filter banks. Fig. 2.1(b), in its turn, demonstrates inverse discrete wavelet transform. Here  $H_0(z)$  is a transfer function of approximation (lowpass) filter, and  $H_1(z)$  – detail (highpass) filter transfer function. At the outputs of the filters from input samples  $x[i]$  the output samples of, accordingly, approximation coefficients  $a[k]$  and detail coefficients  $d[k]$  are formed. In order to keep the total number of samples without changes, the number of coefficients must be twice as small, which can be achieved by performing a downsampling operation ( $\downarrow 2$ ) by keeping only odd (or even) numbered

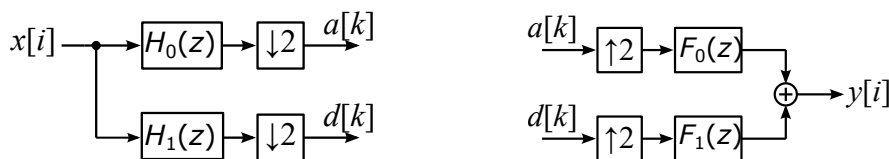


Fig. 2.1. Discrete wavelet transform with filter banks: a) direct, b) inverse.

samples of signal. This choice affects the result of transform, since the values of coefficients in these two cases are different. During the simulation it has been determined that when odd numbered samples are kept, during the reconstruction with filter bank shown in Fig. 2.1(b), the reconstructed signal has shorter delay by 1 sample time interval compared to reconstruction from even numbered samples.

For perfect reconstruction  $H_0(z)$  and  $F_0(z)$ , as well as  $H_1(z)$  and  $F_1(z)$  must be mutually orthogonal. Furthermore,  $H_0(z)$  and  $H_1(z)$  separate different frequency bands – one filter is for lowpass band ( $H_0(z)$ ) and another – for highpass band ( $H_1(z)$ ). In such a case, transfer functions of all four filters can be expressed from  $H_0(z)$ :

$$H_1(z) = z^{-N} H_0(-z^{-1}), \quad (2.1)$$

$$F_0(z) = z^{-N} H_0(z^{-1}), \quad (2.2)$$

$$F_1(z) = -H_0(-z), \quad (2.3)$$

where  $N$  is the order of filter. The filter pair  $H_0(z)$  and  $H_1(z)$  forms analysis filter bank, which performs signal decomposition into coefficients, while filter pair  $F_0(z)$  and  $F_1(z)$  forms synthesis filter bank, which performs signal reconstruction from coefficients. In this Doctoral Thesis, Daubechies-3 discrete wavelets [12] have been used as a popular choice in applications. In the created programs it is possible to specify impulse responses of any other wavelet filters, if necessary. The coefficients of the Daubechies-3 wavelet transfer functions are the following:

Table 2.1. Coefficients of Daubechies-3 Discrete Wavelet Filter Bank Transfer Functions

$h_0[k]$	{0.0352 -0.0854 -0.1350 0.4599 0.8069 0.3327}
$h_1[k]$	{-0.3327 0.8069 -0.4599 -0.1350 0.0854 0.0352}
$f_0[k]$	{0.3327 0.8069 0.4599 -0.1350 -0.0854 0.0352}
$f_1[k]$	{0.0352 0.0854 -0.1350 -0.4599 0.8069 -0.3327}

The analysis filter bank is formed of two FIR filters with impulse responses specified by two first rows of Table 2.1. The synthesis filter bank is not required for Hurst parameter estimation. Considering the fact that these two FIR filters have common input, it is possible to merge delay units of the filters and create a filter bank with diagram shown in Fig. 2.2.

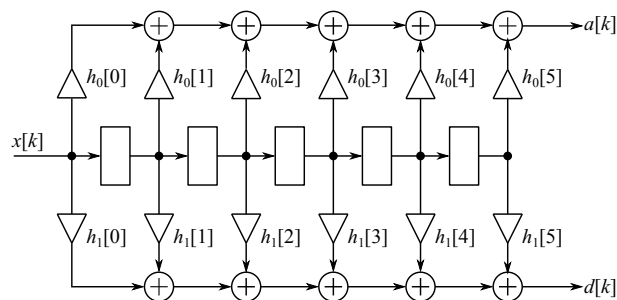


Fig. 2.2. Digital filter bank with merged delay line for Daubechies-3 wavelets.

Fig. 2.2 shows direct implementation of discrete wavelet transform with filter banks, assuming that a downsampling operation ( $\downarrow 2$ , not specified in the figure) for coefficients  $a[k]$  and  $d[k]$  will be performed separately after filtering. It is inefficient, since the half of the filtered values are calculated and then ignored. A more efficient solution – polyphase filter bank structure shown in Fig. 2.3.

The polyphase filter bank signal is divided into even and odd numbered samples, and each component is separately filtered by the polyphase filter bank. The total number of calculations

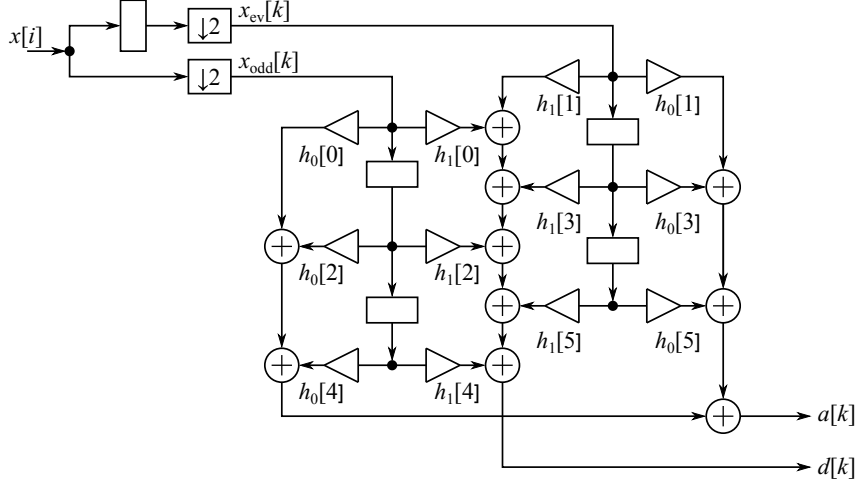


Fig. 2.3. Polyphase filter bank implementation with odd numbered samples after downsampling.

per filtering operation is the same for one signal sample; however, considering the fact that only a half of the samples will be processed (the downsampling  $\downarrow 2$  here is performed before filtering), the total number of samples is also only a half of the input signal samples.

According to the filter bank structure shown in Fig. 2.3, the program in high-level programming language has been written, which implements the algorithm of real-time discrete wavelet transform with the polyphase filter bank. This algorithm is shown in Fig. 2.4, assuming that a downsampling operation keeps odd numbered samples.

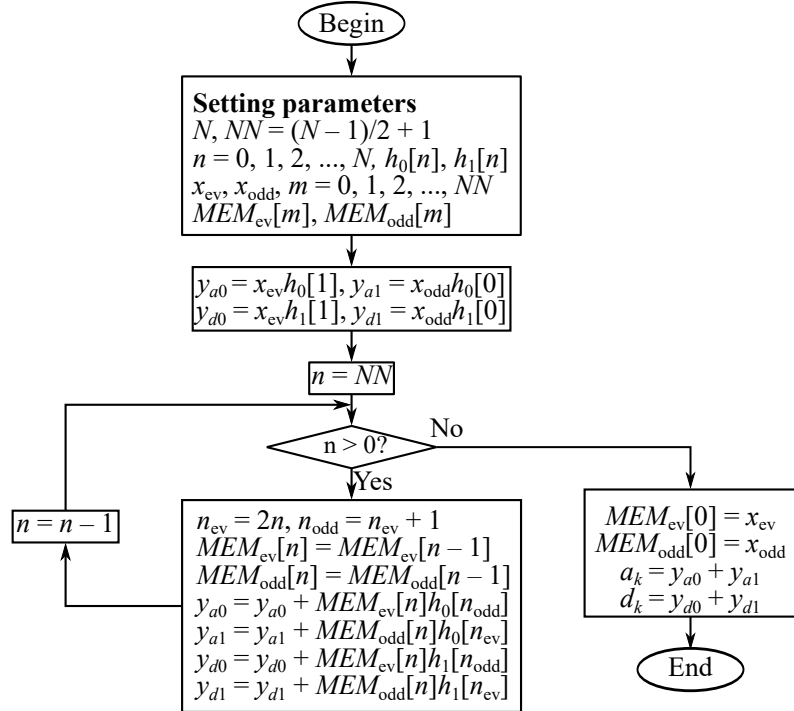


Fig. 2.4. Polyphase implementation of the filter bank with odd numbered samples.

Fig. 2.4 illustrates the algorithm for a single-scale discrete wavelet transform. In order to calculate transform for a greater number of scales, the previous scale approximation coefficients  $a_{j-1}[k]$  must be used as an input signal for very same filter bank of the next scale transform, which will result in next scale approximation coefficients  $a_j[k]$  and detail coefficients  $d_j[k]$ .

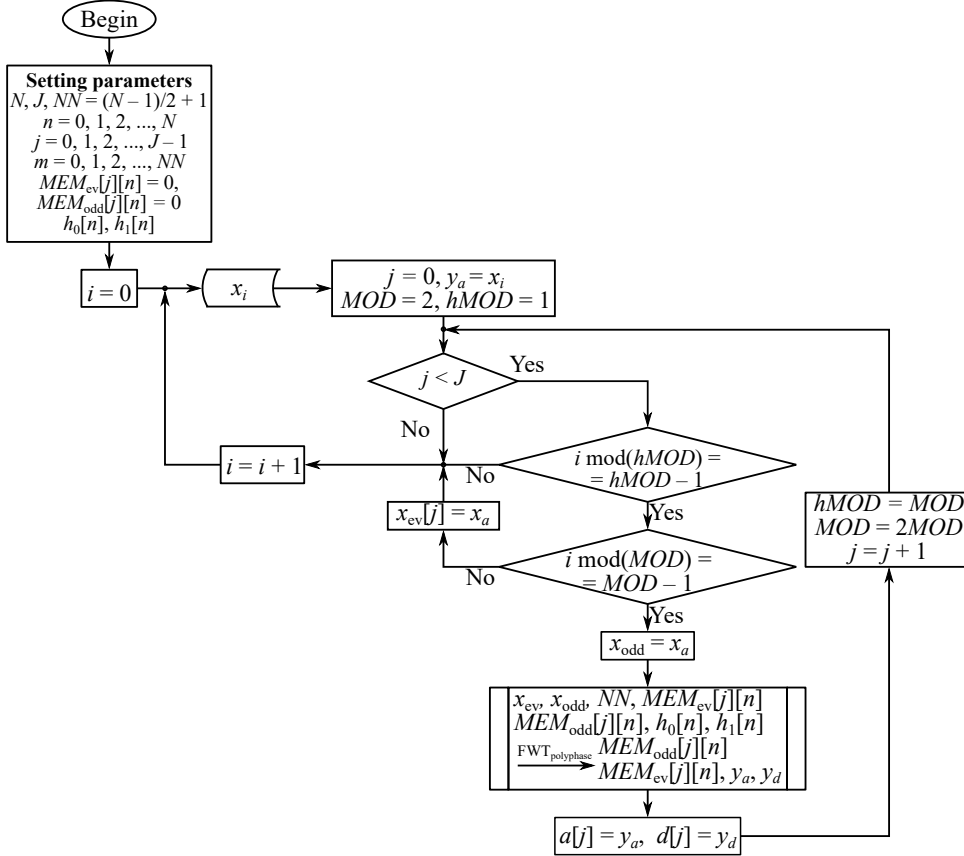


Fig. 2.5.  $J$  scale real-time fast discrete wavelet transform algorithm with the polyphase filter bank for odd numbered samples.

Such polyphase structure implementation has two times higher performance compared to direct implementation of discrete wavelet transform in Fig. 2.2. The polyphase filter bank can be improved further to the lattice structure filter bank with even greater performance potential.

## 2.3 Traffic Self-Similarity Parameter Estimation, Implementation with Filter Banks and Estimation Error

Very often discrete wavelet transform is calculated repeatedly. In such a case, for next discrete wavelet transform scale  $WT^{(j)}$  the input signal is represented by approximation coefficient samples  $\{a_{j-1,k}\}$  of scale  $WT^{(j-1)}$ , and such a process can be recursively repeated upon an affordable result or unless the set of approximation coefficients  $\{a_{j,k}\}$  becomes too short to perform further decomposition. Such a way, after  $J$  scale discrete wavelet transform the total result consists of:

- the largest scale  $J$  approximation coefficient set  $\{a_{J,k}\}$ ;
- detail coefficient sets for every analysed scale:  $\{d_{J,k}\}, \{d_{J-1,k}\}, \dots, \{d_{1,k}\}$ .

This way the result of discrete wavelet transform for scale  $J$  consists of  $K$  samples. Such recursive discrete wavelet transform is a base for network traffic self-similarity parameter  $H$  estimation: for every current scale the analysed frequencies are decreased twice. If the analysed process is self-similar, i.e. it has similar behaviour over different time scales, the detail coefficients are bound to indicate that fact.

Such self-similarity is represented by detail coefficient power  $D_j$ , where  $j$  is the number of current scale, i.e. the number of current discrete wavelet transform level. This power can be calculated according to (3.1) and it increases exponentially over each scale at a constant increase rate.

$$D_j = \frac{1}{n_j} \sum_{k=1}^{n_j} d_{j,k}^2, \quad (3.1)$$

where  $j$  is the number of scale for which power  $D_j$  is calculated,  $d_{j,k}$  – detail coefficients  $d_k$  of respective scale and  $n_j$  – the number of such coefficients at scale  $j$ .

Fig. 3.1 shows  $\log_2(D_j)$  relationship to scale number with separate dots, each of them corresponds to logarithm of detail coefficient power at scale  $j$ . After linear interpolation of this relationship, it is possible to determine slope  $a$ , which can be used according to:

$$a = 2H - 1, \quad (3.2)$$

for self-similarity parameter  $H$  evaluation. Fig. 3.1 shows the logarithm of detail coefficient power  $\log_2(D_j)$  relative to scale number for Pareto random process with self-similarity parameter  $H = 0.8$ . As a result of such relation approximation, the following expression has been obtained:  $\log_2(D_j) = 0.6024j + 7.329$ , according to which for slope parameter of  $a = 0.6024$ , by using (3.2), the self-similarity parameter value can be estimated  $\hat{H} = (a + 1)/2 = 0.8012$ . This value is very close to the specified value during simulation of  $H = 0.8$ .

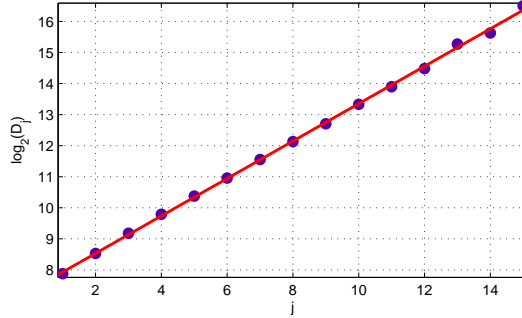


Fig. 3.1. Logarithm of detail coefficient power  $\log_2(D_j)$  relative to scale  $j$ .

For evaluation of relationship slope parameter  $a$ , the Least squares method is well suited (3.3):

$$a = \frac{\sum_{j=1}^J j^2 \sum_{j=1}^J \log_2(D_j) - \sum_{j=1}^J j \sum_{j=1}^J j \log_2(D_j)}{J \sum_{j=1}^J j^2 - \left( \sum_{j=1}^J j \right)^2}, \quad (3.3)$$

where  $j$  is the number of scale, for which power  $D_j$  is being evaluated and  $J$  is the number of such scales.

After describing self-similarity parameter  $H$  estimation algorithm, the *Matlab* function has been created, which performs discrete wavelet transform with Daubechies-3 wavelets and filter bank approach (Figure 2.1(a)) and Hurst parameter  $H$  estimation function. With this function it is possible to estimate self-similarity parameter  $\hat{H}$  average value, and the number of total scales  $J$  can also be specified. The parameter is estimated over all scales up to specified number<sup>3</sup>.

<sup>3</sup>Naturally, the minimal number of scales for such estimation is 2, thus at least for 2 scales the discrete wavelet transform has to be calculated. This is explained by a minimal number of points required for approximation of linear function.

For purpose of studying of the number of discrete wavelet transform scales, transform window length and its relationships to traffic self-similarity parameter  $H$ , the program in *Matlab* has been created. This program estimates self-similarity parameter  $\hat{H}$  and absolute estimation error  $\Delta H = |\hat{H} - H|$  for different transform window lengths and considers different numbers of the scales. The purpose is to define the measure of the influence for these parameters on estimation accuracy and how this accuracy depends on these parameters, if the value of estimated parameter  $H$  changes.

The self-similar traffic is formed as the number of requests per time interval  $\Delta t$ , where intervals between requests are generated with Pareto distributed random numbers. If the current request exceeds the interval of measurement  $\Delta t$ , then it is counted at the next measurement period. Such traffic has been saved as files for further postprocessing and analysis. For all simulations the traffic being used has measurement interval of  $\Delta t = 1$  and intensity  $\lambda = 50$ , while total volume of traffic consists of  $T = 2^{24} \Delta t$  units. There are two series of the simulation measurements:

- traffic analysis for self-similarity parameter values in range  $0.5 < H < 0.99$  with increment step of 0.1;
- traffic analysis for self-similarity parameter values in range  $0.8 < H < 0.99$  with increment step of 0.05.

The traffic has been processed by segments with lengths from  $M_{\min} = 2^{10} = 1\,024$  to  $M_{\max} = 2^{24} = 16\,777\,216$ , and after every increase of segment length for 2 times the maximum number of scales has also been increased by 1.

The results of described simulations are summarised in appendices of the Doctoral Thesis. These tables can be used to construct graphs of self-similarity parameter estimated average value  $\hat{H}$  and average absolute error  $\Delta H$  relative to number of the scales  $J$  for various segment length values (the segment length is increased from left side to the right, starting from top and continuing to bottom).

The analysis of the results shows that it is difficult to accurately estimate self-similarity parameter for low (i.e.,  $H = 0.5$ ) and high ( $H > 0.9$ ) values, while values in the range of  $H = 0.8$  (Figure 3.2) can be estimated with high accuracy.

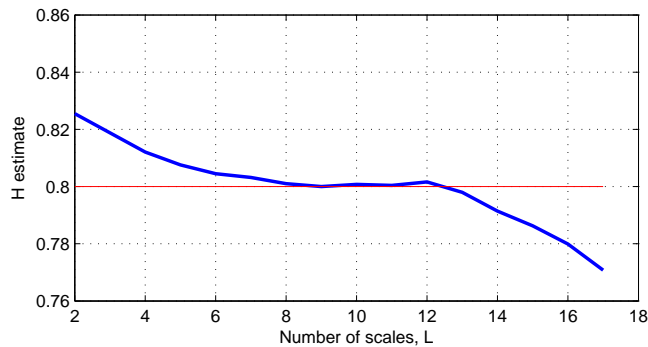


Fig. 3.2.  $\hat{H}$  estimate for  $H = 0.8$  and segment length  $M = 2^{21}$ .

It is interesting that for values in range  $0.7 < H < 0.8$  the optimal number of scales is discovered, and for case of  $H = 0.8$  the interval of these optimal values is wider (see Fig. 3.2). This proves that a maximum number of scales used for estimation, i.e. calculation of discrete wavelet transform for such number of scales, is not necessarily the best option. However, at the same time, in case of segment length increase a higher number of scales has to be used to maintain accuracy at the same level.

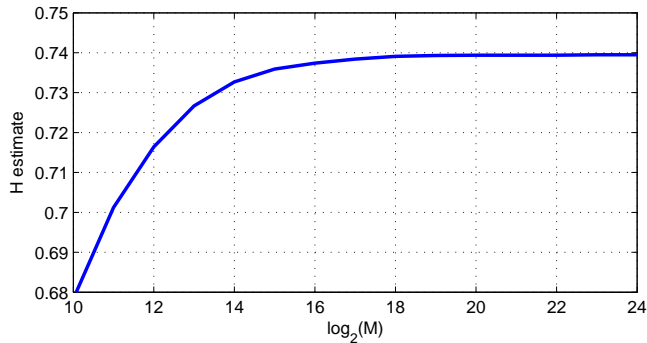


Fig. 3.3. Self-similarity parameter estimate  $\hat{H}$  relative to segment length logarithm for  $H = 0.7$  and  $J = 7$  scales.

Furthermore, the case when number of scales  $J$  is constant for various values of the segment length has been studied. This means that by increasing the length of the segment  $M$ , the new scales are ignored and previous number of scales is being kept instead. Very interesting that in such a case, regardless of specified Hurst parameter  $H$  and length of the segment, meaning in all cases without exceptions, the resulting behaviour is the same as shown in Fig. 3.3. This means that for every scale there is an accuracy limit and, in order to increase the accuracy, it is insufficient just to increase the segment length, but also a higher number of scales has to be used.

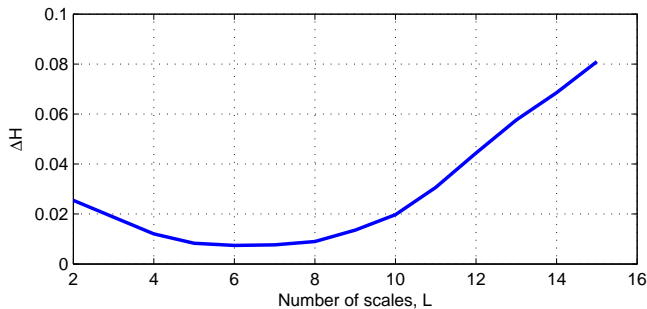


Fig. 3.4. Average absolute error  $\Delta H$  for  $H = 0.8$  and segment length  $M = 2^{15}$ .

By analysing self-similarity parameter  $\hat{H}$  estimate average error  $\Delta H$ , it can be concluded that starting with specific segment length  $M_0$  for value of  $H = 0.8$  the error relationship to number of the scales  $J$  has a minimum<sup>4</sup> (see Fig. 3.4), and this behaviour is preserved for all values of the segment length  $M > M_0$ . For values  $H < 0.8$  the behaviour of error relationship has a negative slope (decrease), while for values  $H > 0.8$  the behaviour of the error has a positive slope (increase).

The simplified Hurst parameter estimation diagram is shown in Fig. 3.5. It is based on discrete multi-scale wavelet transform from Fig. 2.5. This implementation uses the polyphase filter bank; however, if it is necessary, it can be easily switched over to the lattice filter bank.

The algorithm shown in Fig. 3.5 for every traffic sample (for example, this can be packet count per time unit) calculates discrete wavelet transform in real-time and saves detail coefficients of total number LEN per one scale. As it has been mentioned before, the number of scales  $J$  has a great impact on Hurst parameter estimation accuracy and this value in the algorithm can be specified and modified during execution in order to adapt to Hurst parameter changes. If detail coefficient power values have been evaluated, i.e. algorithm processed the last analysed

<sup>4</sup>Traffic with  $H = 0.8$  has been generated repeatedly for two times, and in both attempts the results were the same, even the minimal length of segment  $M_0$  in these experiments was the same.

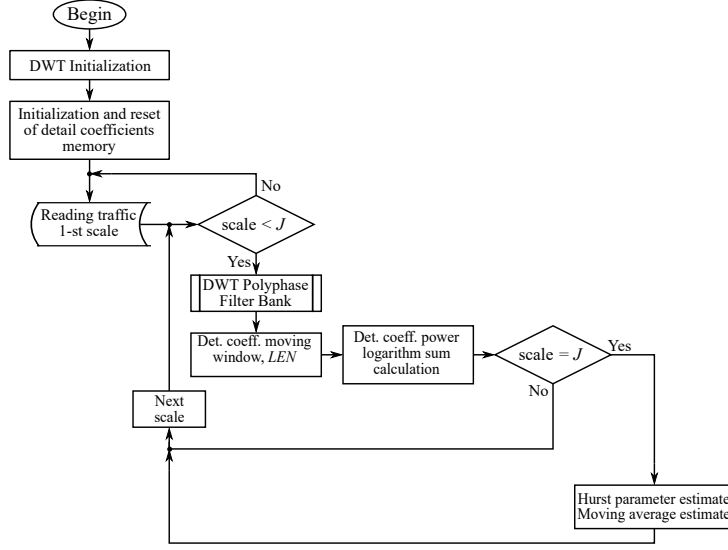


Fig. 3.5. Hurst parameter estimation algorithm with the polyphase filter bank, simplified diagram.

scale  $j = J$ , the Hurst parameter value can be estimated. For this purpose, the least squares method can be used according to (3.3) to calculate the slope for average power logarithm relative to the number of scale.

In addition to the Hurst parameter momentary value, the average value is also estimated by moving average. The length of the moving average window  $AVG\_LEN$  according to the expression:

$$E[\hat{H}] = \frac{AVG\_LEN \cdot E[\hat{H}] + \hat{H}[k] - \hat{H}[k - 1]}{AVG\_LEN}, \quad (3.4)$$

where  $\hat{H}$  is Hurst parameter estimate and  $E[\hat{H}]$  – the average value of such estimate. These Hurst parameter momentary and average values are calculated per every traffic input sample and represent the final goal of the described algorithm for estimator.

Table 3.1. Self-Similarity Parameter Estimation for Different Scales  $j$ ,  $J_{\max} = 8$

Scale, $j$	Processing time	DWT processing time
2	0.021 s	0.0197 s
3	0.0203 s	0.0198 s
4	0.02 s	0.0195 s
5	0.0202 s	0.0203 s
6	0.021 s	0.0198 s
7	0.021 s	0.02 s
8	0.021 s	0.0204 s

Table 3.1 summarizes data for PC with *Core i5-4690* processor, clock frequency 3,2 GHz. As it can be seen from the results, the processing time increases insignificantly compared to discrete wavelet transform calculation.

However, here it is necessary to account for the fact that traffic values have been read from hard disk drive with much lower performance and data read speed than performance of CPU (the computer has high performance SSD hard disk drive). In order to estimate the performance of algorithm itself excluding the time costs of data read process, the discrete wavelet transform has been calculated for sample number  $i$  instead (which is variable in the register memory) and

self-similarity parameter of such “traffic” has been evaluated. The results are the following:

- Discrete wavelet transform calculation time is 0.000239273 s;
- Hurst parameter estimate calculation time<sup>5</sup> is 0.000564183 s.

Results show that, overall, Hurst parameter estimation requires almost the same time, which is required to perform discrete wavelet transform over  $J$  scales with the polyphase filter bank.

## 2.4 Packet Loss Probability Analysis for Generated Self-Similar Traffic in $P/M/1/K$ and $G/M/1/K$ Simulation Models

This chapter describes multiple experiments, in which traffic has been simulated for various utilisation coefficient  $\rho$  and Hurst parameter  $H$  values. The main purpose of the series of experiments is to determine average queue length  $E[R]$  and maximum queue length  $\max(R)$ , compare these two measures and study the relationship between them and the Hurst parameter  $H$  values. Furthermore, these values of average queue length  $E[R]$  will be used in  $G/M/1/K$  and  $P/M/1/K$  models with limited buffer memory capacity. The volume of buffer memory is limited by average queue length  $E[R]$  and multiples of this value, such as triple queue length  $3E[R]$ , and so on. During the simulation process packet loss probability  $P_{\text{loss}}$  is estimated and after the experiments the relationship between this probability and Hurst parameter  $H$  is studied.

By using *Matlab Simulink* modelling tool the model  $P/M/1$  has been created with unlimited buffer memory capacity. The parameters of created model are as follows:

- Traffic intensity  $\lambda = 100$  packets/s, or average request inter-arrival time is  $T_a = 1/120$  s, the intervals are Pareto distributed.
- Traffic self-similarity (Hurst) parameter  $H$  specified in the range from 0.6 to 0.95 with step of 0.05.
- Total number of the requests in simulation is 1000 000.
- The performance of processing node is  $\mu = 125$  packets/s, or average processing time is  $T_s = 1/125$  s, processing time intervals are exponentially distributed.

Thus, the described model has been researched for utilisation coefficient value  $\rho = \lambda/\mu = 0.8$ . Such a value has been chosen intentionally, since it corresponds to a medium point in the utilisation coefficient range of real systems. Utilisation coefficient of real systems, for them to operate efficiently, must be within the range  $0.7 \leq \rho \leq 0.9$ . As a result, for every Hurst parameter  $H$  value the average queue length  $E[R]$  and maximum queue length  $\max(R)$  have been evaluated. In order to determine for every Hurst parameter ht ratio between average queue length  $E[R]$  and maximum queue length  $\max(H)$ , and evaluate dependency of this ratio on the Hurst parameter value, the graph of such a ratio has been constructed and it is shown in Fig. 4.1.

Fig. 4.1 describes relationship between this ratio and the Hurst parameter. The ratio decreases for higher values of the Hurst parameter. This can lead to a conclusion that the higher traffic self-similarity measure, the closer average queue length to maximum queue length. However, this relationship is not monotonous, as it can be seen in the range of  $H = 0.8$  where the behaviour of graph has changed and ratio is increasing.

The similar results have been obtained for three traffic generation models:

1.  $P/M/1$  model with Pareto distributed inter-arrival time intervals;

---

<sup>5</sup>Which, obviously, includes discrete wavelet transform processing time.

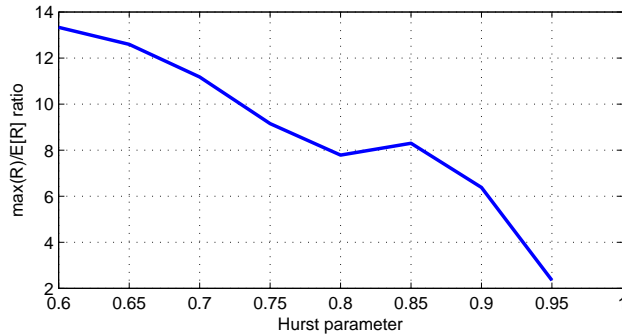


Fig. 4.1. GPSS  $P/M/1$  model maximum queue length  $\max(R)$  to average queue length  $E[R]$  ratio.

2.  $P/M/1$  with ON/OFF traffic and Pareto distributed inter-arrival time intervals;
3.  $G/M/1$  model with Weibull distributed inter-arrival time intervals.

The average and maximum queue length values have been evaluated for every model with multiple values of utilisation coefficient achieved by modifying traffic intensity parameter  $\lambda$ :

1.  $\lambda = 75$  pck/s and utilization coefficient of  $\rho = 0.6$ ;
2.  $\lambda = 87.5$  pck/s and utilization coefficient of  $\rho = 0.7$ ;
3.  $\lambda = 100$  pck/s and utilization coefficient of  $\rho = 0.8$ ;
4.  $\lambda = 112.5$  pck/s and utilization coefficient of  $\rho = 0.9$ .

The simulations have been executed for  $P/M/1$ ,  $P/M/1$  with ON/OFF traffic and  $G/M/1$  queuing models in *Matlab*. In this program the values of parameters have been changed, the simulations have been executed and resulting data have been saved as files. These files have been used for plot construction, the example of such plots is shown in Fig. 4.2 for  $P/M/1$  model. For models with other traffic generation model there are similar results.

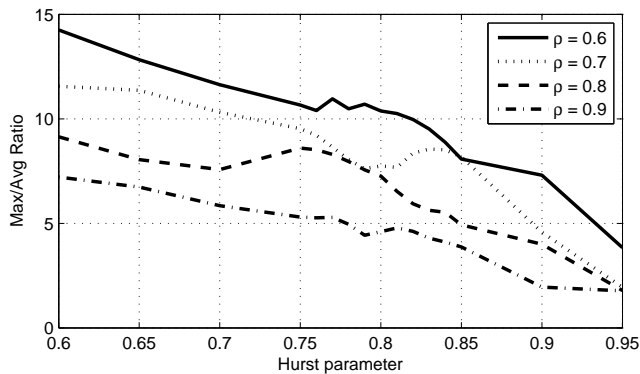


Fig. 4.2. Ratio of maximum  $\max(R)$  and average  $E[R]$  queue length for *Simulink* model depending on Hurst parameter  $H$  for various utilisation coefficients  $\rho$ .

In order to estimate packet loss probability  $P_{\text{loss}}$ , the buffer memory of model must be limited from above. This volume is to be specified in simulation as specific number. The studies made show that the volume does depend both on Hurst parameter  $H$  and utilisation coefficient  $\rho$ . [35] proposes expression for buffer memory volume estimate calculation; however, in previous experiments it has been observed that this expression cannot be applied. There are

recommendations provided on choice of buffer memory volume in [15], but during the following experiments the volume of buffer memory has been chosen to be multiple of average queue length  $E[R]$  with constant multiplier  $k$  according to (4.1). In the present Doctoral Thesis  $k$  is an integer number in range from 1 to 10:

$$K = k \cdot E[R], \text{ where } k = 1, 2, 3, \dots \quad (4.1)$$

After simulations and analysis of the results it can be concluded that the buffer memory volume change leads to packet loss probability  $P_{\text{loss}}$  value change. However, comparing values evaluated in the same Hurst parameter range of  $0.6 \leq H \leq 0.95$  and the same utilisation coefficients, the following can be observed:

- $P_{\text{loss}}$  values are changing (specifically – logarithmic values  $\lg P_{\text{loss}}$ );
- the general behaviour of plot curve remains same.

Thus, the results of simulations show that the choice of buffer memory volume affects  $P_{\text{loss}}$  values more than dynamics of  $P_{\text{loss}}$  changes depending on Hurst parameter  $H$ . Utilisation coefficient  $\rho$  also greatly influences behaviour of such changes; however, for the same utilisation coefficient values at different buffer memory volume the form of curve remains similar. Such results are valid for 3 described models:  $P/M/1/K$ ,  $P/M/1/K$  with ON/OFF traffic and  $G/M/1/K$  with Weibull distribution law.

For greater observability the results can be represented in 3D-plot form as surface, representing the packet loss probability logarithm relation to Hurst parameter  $H$  and utilisation coefficient  $\rho$ . This allows visual concluding on minimum value existence for such surface at specific values of Hurst parameter  $H$  and utilisation coefficient  $\rho$ . The example of such 3D-surface is shown in Fig. 4.3 for  $P/M/1/K$  model with  $K = 3E[Q]$

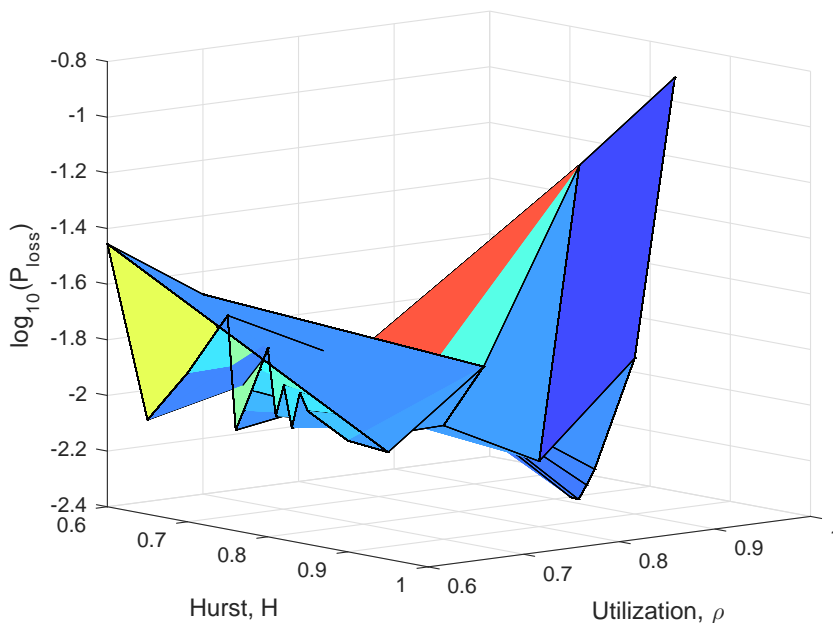


Fig. 4.3. *Simulink*  $P/M/1/K$  queuing model packet loss probability logarithm  $\lg P_{\text{loss}}$  in relation to Hurst parameter  $H$  and utilisation coefficient  $\rho$  values.

For other traffic models such minimums exist as well and, accordingly, such parameters, for which this minimum can be observed, regardless of buffer memory volume  $K$  factor  $k$ . For

every specific model this minimum is different; however, in all cases the values of parameters are close to 1 rather than 0.5. For instance, in case of  $P/M/1/K$  model such parameter values are  $H \approx 0.9$  and  $\rho \approx 0.8$ .

In order to determine such parameters, i.e. find a solution to an optimisation task, Bellman algorithm [4] can be applied, which can be used to estimate sequence of decisions on system parameters  $K$  and  $\rho$  choice for specific  $H$  parameter value in order to provide the minimum of packet loss probability  $P_{\text{loss}}$  and optimal solution within total cost criteria. The dynamic programming principle itself has no relation to program code writing, i.e. programming in usual meaning. Instead, the optimisation procedure is performed, in which for every approximation the better solution is determined, unless requirements for one of the parameters are exceeded.

In order to apply the dynamic programming Bellman algorithm, it is necessary to summarise experimental data in table for a single value of  $H$  parameter value, for which an optimisation task is solved. These values were collected from series of simulations and included packet loss probability  $P_{\text{loss}}$  values for various values of Hurst parameter  $H$ , utilisation coefficient  $\rho$  and buffer memory volume  $K$ . In order to provide continuous variation of the last mentioned value, there were additional simulations performed with buffer memory volumes  $2E[R]$  and  $4E[R]$ , as well as  $6E[R]$ ,  $7E[R]$ ,  $8E[R]$ ,  $9E[R]$  and  $10E[R]$ .

	$\rho = 0.6$	$\rho = 0.7$	$\rho = 0.8$	$\rho = 0.9$
$K = 1E[R]$	1 6 0.10748	1 7 0.075375	1 8 0.057081	1 9 0.029627
$K = 2E[R]$	2 6 0.042893	2 7 0.026055	2 8 0.020595	2 9 0.011168
$K = 3E[R]$	3 6 0.018967	3 7 0.010185	3 8 0.0085718	3 9 0.0048284
$K = 4E[R]$	4 6 0.0084389	4 7 0.0039853	4 8 0.0038761	4 9 0.0023069
$K = 5E[R]$	5 6 0.0038934	5 7 0.0016982	5 8 0.0015656	5 9 0.00099385
$K = 6E[R]$	6 6 0.0018009	6 7 0.00066002	6 8 0.00068674	6 9 0.00045967
$K = 7E[R]$	7 6 0.00080708	7 7 0.00031331	7 8 0.00036305	7 9 0.00021448
$K = 8E[R]$	8 6 0.0004042	8 7 0.00013092	8 8 0.00018028	8 9 0.00011016
$K = 9E[R]$	9 6 0.00019813	9 7 $3.9377 \cdot 10^{-5}$	9 8 $7.5242 \cdot 10^{-5}$	9 9 $5.1062 \cdot 10^{-5}$
$K = 10E[R]$	10 6 $8.9547 \cdot 10^{-5}$	10 7 $1.3647 \cdot 10^{-5}$	10 8 $1.6265 \cdot 10^{-5}$	10 9 $3.0703 \cdot 10^{-5}$

Fig. 4.4. Dominant sequence of Bellman algorithm for  $P/M/1/K$  model with Hurst parameter  $H = 0.8$ .

For every  $H$  parameter value the separate table is created, which summarises packet loss probability  $P_{\text{loss}}$  in relation to utilisation coefficient  $\rho$  and buffer memory volume (or factor  $k$  of this volume). The example of such a table for  $P/M/1/K$  model is shown in Fig. 4.4. For every cell of table, in addition to packet loss probability  $P_{\text{loss}}$  the costs are provided – both for utilisation coefficient  $\rho$  and buffer memory volume  $K$ .

The costs have been estimated as follows:

1. The costs of buffer memory volume  $C_1$  are calculated, assuming the length of packet to be 1500 B according to TCP protocol standard and a maximum number of such packets in memory is multiple of average queue length by factor  $k$ . Thus, the annual costs of 1 MB buffer memory volume can be estimated and total costs can be calculated for 5 years before the hardware ages.
2. The costs of channel data rate  $C_2$  are calculated as percentage of all available channel bandwidth by using traffic intensity value  $\lambda$  and information on packet length. Thus, required bandwidth  $C_{\text{chan}}$  can be estimated with respective actual data rate  $R_{\text{chan}} = \rho C_{\text{chan}}$ , which allows calculating monthly and annual costs to match the time interval of buffer memory service time.

	$\rho = 0.6$	$\rho = 0.7$	$\rho = 0.8$	$\rho = 0.9$
$K = 1E[R]$	172.8 \$ and 0.02 \$ 0.10748 172.82 \$	201.6 \$ and 0.05 \$ 0.075375 201.65 \$	230.4 \$ and 0.13 \$ 0.057081 230.53 \$	259.2 \$ and 0.66 \$ 0.029627 259.86 \$
$K = 2E[R]$	172.8 \$ and 0.04 \$ 0.042893 172.84 \$	201.6 \$ and 0.1 \$ 0.026055 201.7 \$	230.4 \$ and 0.26 \$ 0.020595 230.66 \$	259.2 \$ and 1.32 \$ 0.011168 260.52 \$
$K = 3E[R]$	172.8 \$ and 0.06 \$ 0.018967 172.86 \$	201.6 \$ and 0.15 \$ 0.010185 201.75 \$	230.4 \$ and 0.39 \$ 0.0085718 230.79 \$	259.2 \$ and 1.98 \$ 0.0048284 261.18 \$
$K = 4E[R]$	172.8 \$ and 0.08 \$ 0.0084389 172.88 \$	201.6 \$ and 0.2 \$ 0.0039853 201.8 \$	230.4 \$ and 0.52 \$ 0.0038761 230.92 \$	259.2 \$ and 2.64 \$ 0.0023069 261.84 \$
$K = 5E[R]$	172.8 \$ and 0.1 \$ 0.0038934 172.9 \$	201.6 \$ and 0.25 \$ 0.0016982 201.85 \$	230.4 \$ and 0.65 \$ 0.0015656 231.05 \$	259.2 \$ and 3.3 \$ 0.00099385 262.5 \$
$K = 6E[R]$	172.8 \$ and 0.12 \$ 0.0018009 172.92 \$	201.6 \$ and 0.3 \$ 0.00066002 201.9 \$	230.4 \$ and 0.78 \$ 0.00068674 231.18 \$	259.2 \$ and 3.96 \$ 0.00045967 263.16 \$
$K = 7E[R]$	172.8 \$ and 0.14 \$ 0.00080708 172.94 \$	201.6 \$ and 0.35 \$ 0.00031331 201.95 \$	230.4 \$ and 0.91 \$ 0.00036305 231.31 \$	259.2 \$ and 4.62 \$ 0.00021448 263.82 \$
$K = 8E[R]$	172.8 \$ and 0.16 \$ 0.0004042 172.96 \$	201.6 \$ and 0.4 \$ 0.00013092 202 \$	230.4 \$ and 1.04 \$ 0.00018028 231.44 \$	259.2 \$ and 5.28 \$ 0.00011016 264.48 \$
$K = 9E[R]$	172.8 \$ and 0.18 \$ 0.00019813 172.98 \$	201.6 \$ and 0.45 \$ $3.9377 \cdot 10^{-5}$ 202.05 \$	230.4 \$ and 1.17 \$ $7.5242 \cdot 10^{-5}$ 231.57 \$	259.2 \$ and 5.94 \$ $5.1062 \cdot 10^{-5}$ 265.14 \$
$K = 10E[R]$	172.8 \$ and 0.2 \$ $8.9547 \cdot 10^{-5}$ 173 \$	201.6 \$ and 0.5 \$ $1.3647 \cdot 10^{-5}$ 202.1 \$	230.4 \$ and 1.3 \$ $1.6265 \cdot 10^{-5}$ 231.7 \$	259.2 \$ and 6.6 \$ $3.0703 \cdot 10^{-5}$ 265.8 \$

Fig. 4.5. Dominant sequence of Bellman algorithm for  $P/M/1/K$  model with Hurst parameter  $H = 0.8$  and specified parameter costs.

After calculation of costs, the algorithm shown in Fig. 4.4 can be applied again considering the new values for costs; however, this time the actual price costs are considered instead of some abstract (or relative) values as it has been done the first time. The appendix of the Doctoral Thesis includes tables of dominant sequences for all described in this chapter traffic models:  $P/M/1/K$ ,  $P/M/1/K$  with ON/OFF traffic and  $G/M/1/K$  with Weibull distribution. Hurst parameter values vary in range of  $0.6 \leq H \leq 0.95$  by step of 0.05. In a similar way, Fig. 4.4 shows dominant sequence for Hurst parameter value  $H = 0.8$  considering costs. If during simulation all the packets have been processed, i.e.  $P_{\text{loss}}$  estimation is 0, then such a result is skipped. The example of such a dominant sequence is shown in Fig. 4.5.

For every cell in Fig. 4.5 the separate costs are specified: the costs of channel data rate  $C_2$  and costs of buffer memory  $C_1$ ; the packet loss probability is  $P_{\text{loss}}$  and total costs estimated as sum  $C_2 + C_1$ . The dominant sequence has been created according to the Bellman dynamic programming algorithm and, comparing Fig. 4.4 with Fig. 4.5, the conclusion can be made that a dominant sequence in this case has not been affected by addition of actual price costs, since in both cases the channel data rate cost considerably exceed buffer memory volume cost. Based on table data the plot can be constructed to visualise the relation of total costs  $C_2 + C_1$  to packet loss probability logarithm  $\lg P_{\text{loss}}$  for different values of Hurst parameter  $H$  values. The example of such a plot is shown in Fig. 4.6.

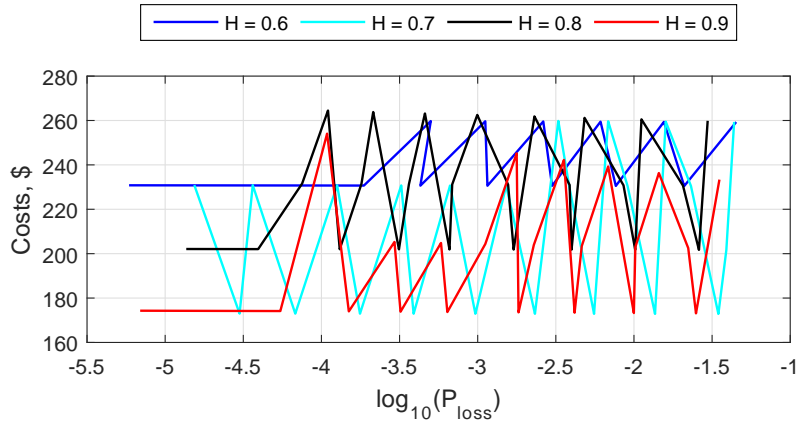


Fig. 4.6. Total costs of  $P/M/1/K$  model related to packet loss probability for different Hurst parameter values.

Based on curves of Fig. 4.6, it can be concluded that minimum costs can be achieved, and the value of these minimum total costs vary, depending on Hurst parameter  $H$  values. This minimums match a set of system parameter values, for which costs can be determined. These minimal costs can be summarised in table and used for router parameter configuration in real-time.

## Main Conclusions

The aims of the Doctoral Thesis have been successfully achieved and all tasks have been accomplished. The results of the research can be summarised by the following conclusions:

- the existing buffer memory volume estimation methods for self-similar traffic do not provide adequate volume estimates and adaptive control of system parameters is necessary, including control of buffer memory volume based on traffic measurements;
- for different Hurst (self-similarity) parameter values the different buffer memory volume corresponds, and, in general, buffer memory volume increase trend can be observed in relation to both the Hurst parameter and utilisation coefficient values;
- the filter bank approach can be used to perform discrete wavelet transform in real-time (including the cases, when no DSP or FPGA is used) with further improvements to the structure, such as polyphase or lattice filter banks;
- the algorithm of discrete wavelet transform implemented in C++ language is fast enough to be used for Hurst parameter estimation in real-time;
- after studying inverse discrete wavelet transform it has been discovered that in order to achieve faster signal recovery it is useful to perform signal downsampling in filter banks such a way that only odd numbered samples remain – this minimises delay at every level (scale) of the transform and as of such – the total delay of signal reconstruction over all of the scales;
- the Hurst parameter estimator can be created in such a way that it renews Hurst parameter estimates for every traffic sample at the input, performing multi-scale analysis and calculation time is comparable to discrete wavelet transform calculation time, meaning that such estimator can be practically used;
- the Hurst parameter measurement precision can be improved by a choice of specific number of analysed scales, which is lower than a full number of analysed scales. The algorithm proposed can be extended to have adaptive control for a number of scales during execution;
- when estimating packet loss probability for the system with limited buffer memory, it has been observed that for an adaptive choice of buffer memory amount the Hurst parameter increment does not necessarily increase packet loss probability. For example, for Hurst parameter values in the range of  $0.8 \leq H \leq 0.9$  the opposite has been observed;
- self-similar traffic with Hurst parameter  $H = 0.8$  or close to this value has abnormal behaviour for multiple relationships, such as average/maximum queue length relation to the Hurst parameter, or Hurst parameter estimated error relative to process actual Hurst parameter value. In many publications, the examples are provided for this value of  $H = 0.8$ , which corresponds to medium self-similarity magnitude;
- the obtained Hurst parameter, buffer memory volume and packet loss probability measurements can be used to perform multi-parameter optimisation with the Bellman dynamic

programming algorithm for different criteria: total costs, packet loss probability minimum, and so on;

- Bellman algorithm application for self-similar network traffic with real bandwidth and buffer memory volume costs taken into account show that by the end of 2013 the buffer memory volume must be increased and utilisation coefficient must be decreased in order to minimise total resource costs;
- dominant sequence graphs show total costs relative to packet loss probability, and for Hurst parameter value of  $H = 0.8$  the behaviour of curve is also different compared to curves of other Hurst parameter values and it has resulted in too high costs.

The main results of the Doctoral Thesis have been described in publications and presented at international conferences.

## REFERENCES

- [1] P. Abry, D. Veitch. Wavelet-Analysis of Long-Range-Dependent Traffic // IEEE Transactions on Information Theory. - IEEE Computer Society Washington, DC, USA, 1998 – vol. 44, no. 1 - pp. 2–15. DOI: 10.1109/18.650984
- [2] Amin, F.; Mizanian, K. Buffer management for self-similar network traffic. // Telecommunications (IST), 2012 Sixth International Symposium, 6–8 Nov. 2012 – pp. 737–742
- [3] Amin, F.; Mizanian, K.; Mirjalily, G. Active queue management for self-similar network traffic // Electrical Engineering (ICEE), 2013 21st Iranian Conference on , vol., no., 14–16 May 2013 – pp. 1–5
- [4] Richard Bellman. Dynamic Programming. // Princeton University Press. – NY, USA, 1957 – 340 p.
- [5] Florian Bomers. Wavelets in real time digital audio processing: Analysis and sample implementations. Master's Thesis. // University of Mannheim, May 2000 – 119 p.
- [6] Bregni, S. Compared accuracy evaluation of estimators of traffic long-range dependence. // Communications (LATINCOM), 2014 IEEE Latin-America Conference on , vol., no., 5–7 Nov. 2014 – pp. 1–5
- [7] Gabriel M.de Brito, Pedro B.Velloso, Igor M.Moraes. Information Centric Networks: A New Paradigm for the Internet // Willey-ISTE. – April 2013 – 144 p.
- [8] Chaudhari, S.S.; Biradar, R.C. Resource prediction based routing using wavelet neural network in mobile ad-hoc networks. // Circuits, Communication, Control and Computing (I4C), 2014 International Conference on , vol., no., 21–22 Nov. 2014 – pp. 273–276
- [9] Yiou Chen; Jianhao Hu; Jianrong Wang. Self-similar traffic study of on-chip interconnection networks. // Communications, Circuits and Systems (ICCCAS), 2013 International Conference on , vol. 1, no., 15–17 Nov. 2013 – pp. 381–385
- [10] X.Cheng, K.Xie, D.Wang. Network Traffic Anomaly Detection Based on Self-Similarity Using HHT and Wavelet Transform. // IAS '09. Proceedings of the Fifth International Conference on Information Assurance and Security. – IEEE Press Piscataway, 2009 – pp. 710–713. DOI: 10.1109/IAS.2009.219
- [11] Cisco Identity Services Engine User Guide, Release 1.2 // Cisco Systems, April 7, 2015 – 788 p.
- [12] I. Daubechies and W. Sweldens. Factoring Wavelet Transforms into Lifting Steps. // Fourier Analysis and Applications, 4(3), 1998 – pp. 247–269.
- [13] DeVirgilio, M.; Pan, W.D.; Joiner, L.L.; Dongsheng Wu. Internet delay statistics: Measuring Internet feel using a dichotomous Hurst parameter. // Southeastcon, 2012 Proceedings of IEEE , vol., no., 15–18 March 2012 – pp. 1–6

- [14] Geyong Min; Xiaolong Jin. Analytical Modelling and Optimization of Congestion Control for Prioritized Multi-Class Self-Similar Traffic. // Communications, IEEE Transactions on, vol. 61, no. 1, January 2013 – pp. 257–265
- [15] M. Kulikovs. Research and development of effective managing algorithms in admission control systems for telecommunication networks. Doctoral Diploma Thesis. // Riga: RTU, 2010 – 200 p.
- [16] W. Leland, M. Taqqu, W. Willinger, D. Wilson. On the Self-Similar Nature of Ethernet Traffic // IEEE/ACM Transactions on Networking – IEEE Press Piscataway, vol. 2, no. 1, 1994 – pp. 203–213. DOI: 10.1109/90.282603
- [17] Li, Yongli; Guizhong Liu; Hongliang Li; Hou, Xingsong. Wavelet-based analysis of hurst parameter estimation for self-similar traffic. // Acoustics, Speech, and Signal Processing (ICASSP), 2002 IEEE International Conference on , vol. 2, no., 13–17 May 2002 – pp. 2061–2064
- [18] Liji, P.I.; Dipin, A. Real time data traffic analysis using poisson process in next generation network. // Control, Instrumentation, Communication and Computational Technologies (ICCICCT), 2014 International Conference on , vol., no., 10–11 July 2014 – pp. 289–293
- [19] Mallat, Stéphane. A wavelet tour of signal processing. 2nd edition. // Academic press, 1999 – 668 p.
- [20] B. Mandelbrot. The Fractal Geometry of Nature. // Henry Holt and Company, 1982 – 480 p.
- [21] Mota, Hd.O.; Vasconcelos, F.H.; da Silva, R.M. Real-time wavelet transform algorithms for the processing of continuous streams of data. // Intelligent Signal Processing, 2005 IEEE International Workshop on , vol., no., 1–3 Sept. 2005 – pp. 346–351
- [22] Naornita, C.; Isar, A.; Nelson, J.D.B. Regularised, semi-local hurst estimation via generalised lasso and dual-tree complex wavelets. // Image Processing (ICIP), 2014 IEEE International Conference on , vol., no., 27–30 Oct. 2014 – pp. 2689–2693
- [23] Petiz, I.; Rocha, E.; Salvador, P.; Nogueira, A. Using multiscale traffic analysis to detect WPS attacks. // Communications Workshops (ICC), 2013 IEEE International Conference on , vol., no., 9–13 June 2013
- [24] Premarathne, U.; Premaratne, U.; Samarasinghe, K. Network traffic self similarity measurements using classifier based Hurst parameter estimation. // Information and Automation for Sustainability (ICIAFs), 2010 5th International Conference, 17–19 Dec. 2010 – pp. 64–69
- [25] Z. Prusa and P. Rajmic. Real-Time lifting wavelet transform algorithm // Elektrotechnik. – Brno: International Society for Science and Engineering, o.s., 2011 – vol. 2, no. 3 - pp. 53–59
- [26] David Rincon Rivera. Contributions to the Wavelet-based Characterization of Network Traffic. // PhD Thesis, Program on Telematics Engineering – Universitat Politècnica de Catalunya – Barcelona, July 2007 – 315 p.
- [27] Shu-Yan Chen; Wei Wang; Gao-Feng Qu. Combining wavelet transform and Markov model to forecast traffic volume. // Machine Learning and Cybernetics, 2004. Proceedings of 2004 International Conference on, vol. 5, no., 26–29 Aug. 2004 – pp. 2815–2818

- [28] G. Strang, T. Ngueyen. Wavelets and filter banks. // Wellesley: Wellesley-Cambridge Press, 1996 – 495 p.
- [29] Tereshchenko, T.; Yamnenko, Y.; Veretiuk, A.; Veretiuk, S. Wavelet transform at oriented basis for network traffic forecasting. // Electronics and Nanotechnology (ELNANO), 2013 IEEE XXXIII International Scientific Conference, vol., no., 16–19 April 2013 – pp. 450–454
- [30] Ted Wobber, Thomas L. Rodeheffer and Douglas B. Terry. Policy-based Access Control for Weakly Consistent Replication // Microsoft Research Technical Report MSR-TR-2009-15, – Published February 2009, revised July 2009 – 17 p.
- [31] Yanpu Hu; Wenfu Yang; Yong Wang; Ying Dong. The study of a new Call Admission Control method based on self-similar traffic. // Intelligent Control and Automation (WCICA), 2012 10th World Congress on, vol., no., 6–8 July 2012 – pp. 15–19
- [32] Ye, X.; Xia, X.; Zhang, J.; Chen, Y. Effects of trends and seasonalities on robustness of the Hurst parameter estimators. // Signal Processing, IET , vol. 6, no. 9, Dec. 2012 – pp. 849–856
- [33] Ye Xiaolong; Julong Lan; Wanwei Huang. Network traffic anomaly detection based on self-similarity using FRFT // Software Engineering and Service Science (ICSESS), 2013 4th IEEE International Conference on, vol., no., 23–25 May 2013 – pp. 837–840
- [34] E. Pētersons. Sevīdžīgs trafiks telekomunikāciju un datoru tīklos. // Rīga: RTU Izdevniecība, 2005 – 61 lpp.
- [35] В. Столлингс. Современные компьютерные сети. 2-е издание. // Санкт-Петербург: Питер, 2003 – 783 с.